

Supplementary Information

Universal nanocomposite coating with antifouling and redox capabilities for electrochemical affinity biosensing in complex biological fluids

Aditya Manu Bharti^{1,2, #}, R. K. Rakesh Kumar^{3,4 #}, Cheng-Hsin Chuang^{2,5, *} and Muhammad Omar Shaikh^{6, *}

¹International PhD Program for Science, National Sun Yat-sen University, Kaohsiung 80424, Taiwan.

²Institute of Medical Science and Technology, National Sun Yat-sen University, Kaohsiung 80424, Taiwan.

³Department of Chemical Engineering, National Taiwan University, Taipei City, 10617, Taiwan

⁴Institute of Biomedical Engineering and Nanomedicine, National Healthcare Research institutes, Miaoli County 350, Taiwan

⁵Centre of Excellence for Metabolic Associated Fatty Liver Disease (CEMAFLD), National Sun Yat-sen University, Kaohsiung 80424, Taiwan.

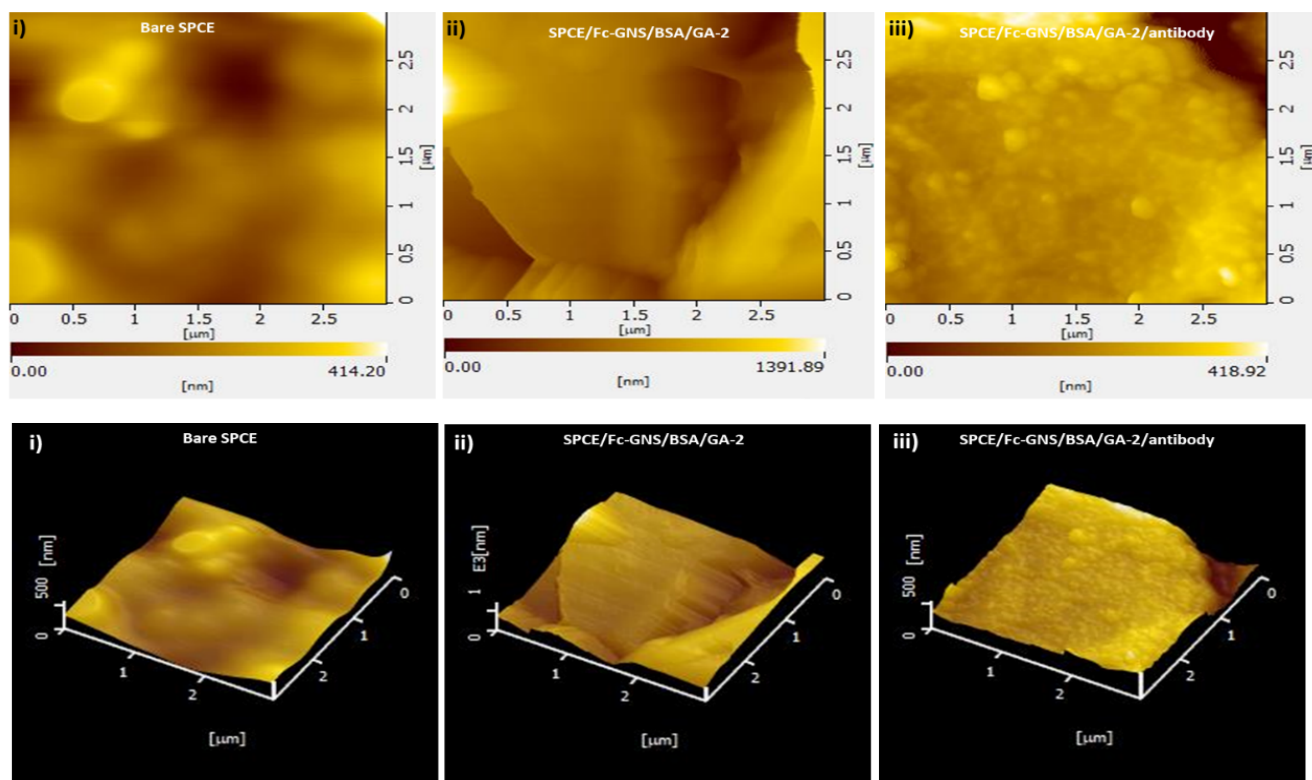
⁶Sustainability Science and Management Program, Tunghai University, Taichung 407224, Taiwan.

* Correspondence Email: chchuang@imst.nsysu.edu.tw; Tel.: +886-75-252-000 ext. 7151

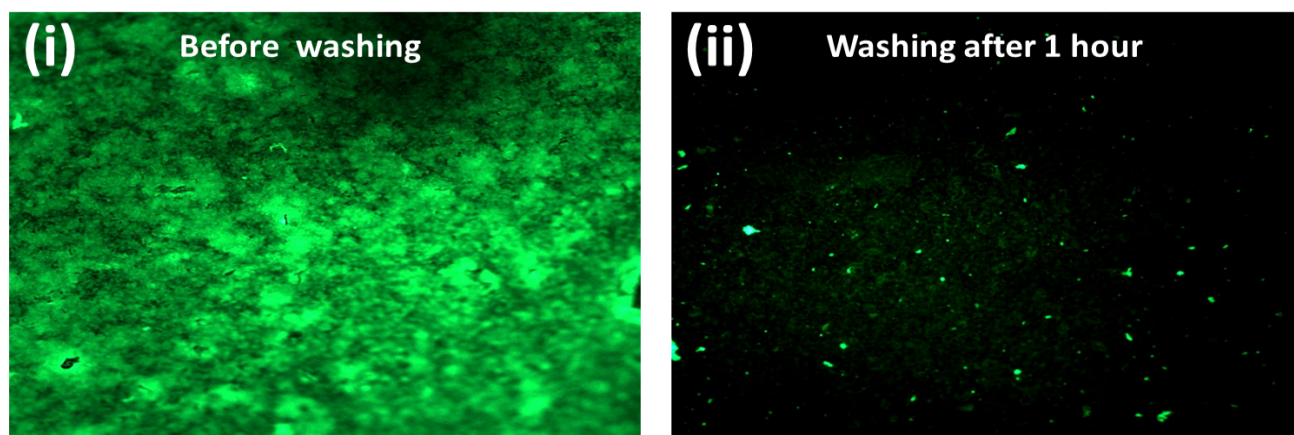
* Correspondence Email: omar@thu.edu.tw; Tel.: +886-4-23590121 ext.39204

Supplementary Figure 1:

AFM pictures to study topography of a) Bare SPCE. b) SPCE/Fc-GNS/BSA/GA. c) SPCE/Fc-GNS/BSA/Antibody.



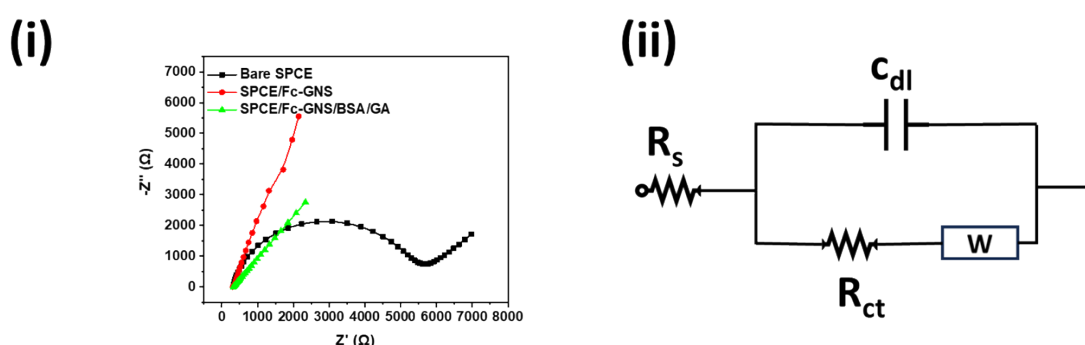
Supplementary Figure 2: Fluorescence microscopy images to confirm covalent immobilization of antibody to SPCE/Fc-GNS/BSA/GA electrode surface.



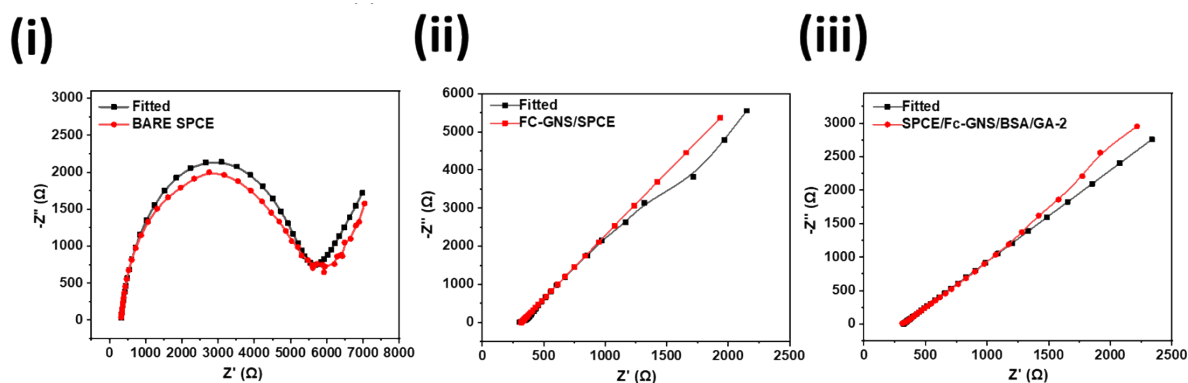
Equivalent Circuit Modelling

An equivalent circuit model was constructed based on the Nyquist plots observed during the EIS investigations in 5 mM $[\text{Fe}(\text{CN})_6]^{+3}/[\text{Fe}(\text{CN})_6]^{+2}$. The equivalent circuit model was then used to simulate the mass transport behaviour of electroactive species at the surface of the bare SPCE and the modified electrodes (SPCE/Fc-GNS and SPCE/Fc-GNS/BSA/GA). The equivalent circuit model consisted of four electrical components, resistance of the solution (R_s), resistance to charge transfer (R_{ct}), Warburg impedance (W) and the double layer capacitance (C_{dl}).

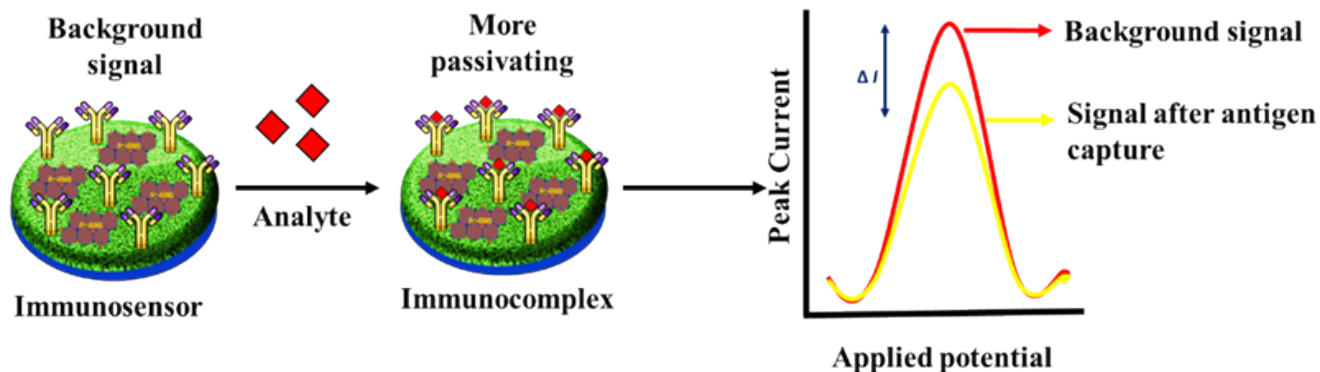
Supplementary Figure 3: (i) Nyquist plots observed during the EIS investigations of SPCE, SPCE/Fc-GNS and SPCE/Fc-GNS/BSA/GA. (ii) The equivalent circuit model representative of the mass transport behaviour of charged species at the surface of the modified electrode.



Supplementary Figure 4: The resulting simulated EIS data in the form of Nyquist plots was fitted and compared against the experimental/observed data, showing good correlation, which confirms the feasibility of the equivalent circuit model to accurately represent the electron transfer kinetics and diffusion characteristics of the modified electrode.



Supplementary Figure 5: Sensing mechanism for immunosensor response.



The observed DPV peak within the potential range of 0.2 to 0.6 V can be attributed to the electro-oxidation of ferrocene (Fc) which is covalently bonded to graphene nanosheets (GNS) to form Fc-GNS. When an applied potential is introduced, ferrocene undergoes electrooxidation, and the released electrons are conducted by the graphene nanosheets to the electrode surface. The Fc-GNS is embedded within the 3D BSA matrix which not only enables anti-fouling capability but also covalent and oriented conjugation of antibodies. BSA, which is inherently passivating in nature, becomes more insulating after the immobilization of antibodies. The SPCE/Fc-GNS/BSA/GA/Antibody configuration serves as the background signal. A subsequent decrease in peak current is observed post-immunosensing due to the formation of an immunocomplex between the antibody and antigen. As the antigen concentration increases, the antibodies at the electrode surface capture more of it, thus impeding electron transport because of the passivating nature of the target antigen (proteins). Consequently, this results in a decrease in peak current. Furthermore, the built-in BSA matrix provides antifouling capabilities to eliminate nonspecific interaction of other interfering proteins to the electrode surface while maintaining the redox capabilities and conductivity due to the embedded Fc-GNS. This ensures highly sensitive and specific affinity biosensing when testing is performed directly in complex biological fluids.

Supplementary Table 1: Fitting values for EIS measurements.

Sample	R_s ($\Omega \text{ cm}^2$)	C_{dl} ($\mu\text{F s}^N$)	W ($\mu\text{F s}^{1/2}$)	R_{ct} ($\Omega \text{ cm}^2$)
Bare SPCE	319	1.59 (N=0.887)	531	5.01
SPCE/FC-GNS	317	257 (N=0.818)	360	7.49
SPCE/FC-GNS/BSA/GA-2	318	386 (N=0.598)	900	1.10 T

Supplementary Table 2: Various electrolytes used for SPCE/Fc-GNS/BSA/GA characterization and immunosensing.

Electrolyte	Artificial Urine	1 M PBS	(0.2) M PBS
--------------------	-------------------------	----------------	--------------------

Conductivity (mS/cm)	23±0.1	14.10±0.2	3.08±0.8
---------------------------------	---------------	------------------	-----------------

Supplementary Table 3: Comparison table highlighting the merits of the developed mediator free electrochemical biosensor over existing

Ref	Bare Electrode	Electrode Material	Sensor type	Detection Range	Sample biofluid	Detection technique (Electrochemical)	Biomarkers	Interference removal step	Redox buffer/ Redox Probe	Target study
[1]	SPCE	rGO	Immunosensor	0.01-200 ng/ml	Serum	DPV	Pepsinogen I	Incubating with BSA (required)	Fe(CN) ₆ ^{3-/4-} (required)	Gastric Cancer
[2]	SCPE	MWCNT	Immunosensor	8–1000 pg/ml	PBS	Amperometry	Interleukin 8	Incubating with BSA (required)	TMB substrate.	Prostate Cancer
[3]	Carbon electrode	(PEDOT)-AuNPs	Aptasensor	0.05–500 ng/ml	Clinical serum	DPV	CEA, NSE antibody	required	Not required (PBS)	Lung Cancer
[4]	LS-graphene	Graphene	Aptasensor	3.75–10 ng/ml	PBS	DPV	AFP, CEA aptamer	Incubating with BSA (required)	Fe(CN) ₆ ^{3-/4-} (required)	Liver Cancer
[5]	GCE	PEDOT-peptide hydrogel	Immunosensor	0.1 ng/mL to 1.0 µg/ml	Human Serum	DPV	HER2	required	Fe(CN) ₆ ^{3-/4-} (required)	Breast cancer
[6]	ITO	Fc-PEI/CNT	Aptasensor	0.2 ng/ml to 1.66 µg/ml	Human serum	DPV	TBA	Incubating with BSA (required)	Not required (PBS)	Lysozyme
This work	SPCE	Fc-GNS/BSA/GA	Immunosensor	0.1 ng/mL to 1.0 µg/ml	Artificial Urine	DPV	IL-8, VEGF (Universal)	Not required (built-in BSA/GA matrix)	Not required (PBS)	Bladder cancer

electrochemical sensors.

Abbreviation used:

ITO - indium tin oxide, SPCE - screen printed carbon electrode, GCE - glassy carbon electrode, LS-Graphene – laser scribed graphene MWCNT - multiwalled carbon nanotube, rGO - reduced graphene oxide, AuNPs - gold nanoparticles, PEDOT - poly(3,4-ethylenedioxythiophene), GNS -graphene nano sheets, PEI – polyethyleneimine, CV - cyclic voltammetry, DPV - differential pulse voltammetry, CEA - carcinoembryonic antigen, VEGF - vascular endothelial growth factor, AFP - α -fetoprotein biomarkers, TBA - thrombin-binding aptamer, DNA aptamer against CEA: 5'-ATA CCA GCT TAT TCA ATT-3, NSE: 5'-CGG TAA TAC GGT TAT CCA CAG AAT CAG GGG-3 NSE4, IL -8 interleukin-8, HER2 -human epidermal growth factor receptor, BSA - bovine serum albumin, PBS - phosphate buffer solution

Normalization of the immunosensor response

The immunosensor response was measured by normalizing the peak current change observed during immunosensing [$\Delta I = I$ after (immunosensing) - I_0 (after antibody immobilization)] with the peak current observed after antibody immobilization [I (after antibody immobilization)] as follows:

$$\text{Normalized immunosensor response } [\Delta I\%] = \frac{\Delta I \text{ (during immunosensing)}}{I_0 \text{ (after antibody immobilization)}} \times 100$$

This method eliminates the analytical concerns of the background signal, thus ensuring that the resulting normalized peak signal variation value is generated solely due to the presence of the analyte.

References

- [1] P. Kanagavalli, S. Eissa, Redox probe-free electrochemical immunosensor utilizing electropolymerized melamine on reduced graphene oxide for the point-of-care diagnosis of gastric cancer, *Talanta*, 270(2024) 125549.
- [2] Y. Wan, W. Deng, Y. Su, X. Zhu, C. Peng, H. Hu, et al., Carbon nanotube-based ultrasensitive multiplexing electrochemical immunosensor for cancer biomarkers, *Biosensors and Bioelectronics*, 30(2011) 93-9.
- [3] Y. Wang, J. Luo, J. Liu, S. Sun, Y. Xiong, Y. Ma, et al., Label-free microfluidic paper-based electrochemical aptasensor for ultrasensitive and simultaneous multiplexed detection of cancer biomarkers, *Biosensors and Bioelectronics*, 136(2019) 84-90.
- [4] Y.-K. Yen, G.-W. Huang, R. Shanmugam, Laser-scribing graphene-based electrochemical biosensing devices for simultaneous detection of multiple cancer biomarkers, *Talanta*, 266(2024) 125096.
- [5] W. Wang, R. Han, M. Chen, X. Luo, Antifouling Peptide Hydrogel Based Electrochemical Biosensors for Highly Sensitive Detection of Cancer Biomarker HER2 in Human Serum, *Analytical Chemistry*, 93(2021) 7355-61.

[6] Y. Du, C. Chen, B. Li, M. Zhou, E. Wang, S. Dong, Layer-by-layer electrochemical biosensor with aptamer-appended active polyelectrolyte multilayer for sensitive protein determination, *Biosensors and Bioelectronics*, 25(2010) 1902-7.